



HAL
open science

Image analysis based real time detection of satellites reception state

D. Attia, C. Meurie, Y. Ruichek, J. Marais, A. Flancquart

► **To cite this version:**

D. Attia, C. Meurie, Y. Ruichek, J. Marais, A. Flancquart. Image analysis based real time detection of satellites reception state. 2010 13th International IEEE Conference on Intelligent Transportation Systems - (ITSC 2010), Sep 2010, Funchal, Portugal. pp.1651-1656, 10.1109/ITSC.2010.5625143 . hal-04757862

HAL Id: hal-04757862

<https://hal.science/hal-04757862v1>

Submitted on 29 Oct 2024

HAL is a multi-disciplinary open access archive for the deposit and dissemination of scientific research documents, whether they are published or not. The documents may come from teaching and research institutions in France or abroad, or from public or private research centers.

L'archive ouverte pluridisciplinaire **HAL**, est destinée au dépôt et à la diffusion de documents scientifiques de niveau recherche, publiés ou non, émanant des établissements d'enseignement et de recherche français ou étrangers, des laboratoires publics ou privés.

IMAGE ANALYSIS BASED REAL TIME DETECTION OF SATELLITES RECEPTION STATE

D. Attia and C. Meurie and Y. Ruichek and J. Marais and A. Flancquart

Abstract—This paper is focused on real time detection of satellite reception state. In constrained environment, such as urban areas, GNSS signals can be received directly, reflected or blocked by obstacles (building, vegetation, etc) and can lead to an error or a lack of positioning. This paper proposes to characterize the GNSS signals reception environment using image analysis. The proposed approach consists of detecting the visible sky part in the images thanks to a k-means based classification algorithm applied in segmented/simplified images. In this paper, two images segmentation/simplification techniques are proposed and compared in terms of robustness, reliability and processing rate. The first one is based on a combination of color and texture information. The second technique uses a geodesic reconstruction by dilatation with an optimal constrast parameter. The main aim of this work consists of determining how many satellites are positioning in the area of visible sky and have a direct reception state. Experimental classification and positioning results, using real data and an evaluation methodology are presented to demonstrate the effectiveness and the reliability of the proposed approach.

I. INTRODUCTION

The positioning function is one of the central functions in ITS (Intelligent Transportation Systems). It is usually provided by a GPS receiver which suffers however of inaccuracy and unavailability in constraints environments due to multi-path or blockage of the signals. The GNSS (Global Navigation Satellite System) panorama will soon be completed by other competitive but interoperable constellations (the modernized Russian GLONASS, the new European Galileo, the Chinese COMPASS) and other Satellite-Based Augmentation Systems (SBAS) that will enhance the global availability and enhance the performance. However, if the global number of satellites received will offer new potentialities, it will not erase the propagation difficulties. Some different levels of work can be chosen to mitigate their impacts: antenna choice, multisensor solution or new correlation techniques, etc. In this paper, we present a solution inspired by land-mobile satellite (LMS) communication studies [1] that aims to detect the satellite state of reception of each signal versus time based on a video record of the surrounding environment. Signals are usually classified in the literature by three states: blocked (no signal received), shadowed (signal attenuated, mainly by vegetation), and direct or clear. In

positioning systems where the main objective of the signal reception is the propagation time estimation, the following three states have been defined [2]: 1/ blocked; 2/ shadowed or alternate path, that represents the case where the signal is received after reflections without any direct ray; 3/ direct. As a comparison with sensor behavior, we can consider that the direct state is the nominal mode, the alternate is a degraded mode and the blocked is a failure. In our study, we focus in particular on the degraded mode which leads to inaccuracy of the positioning result. In order to reduce the lack of performance, some authors chose to exclude the concerned satellites (with shadowed or alternate path) from the positioning computation [3], [4]. But this solution can result in more unavailability. Another approach consists of considering the error bias included by the degraded signal in a new filtering process in order to reduce the error impact without increasing unavailability [5]. The present paper focuses on the detection of the satellites reception state using video analysis of the environment surrounding the GPS antenna. This system has been developed for the first version of the PREDISSAT tool and has inspired other developments with infra-red cameras [4]. The first step of the process concerns image analysis to detect the visible sky and the others objects present in the image. Then, satellites are replaced in the processed image in order to identify whether the signal can be received directly (in a sky region) or not (in a not-sky region). Experimental classification and positioning results, using real data and an evaluation methodology are made to demonstrate the effectiveness and the reliability of the proposed approach. The final goal of this detection will be to apply several solution schemes to enhance accuracy such as exclusion or noise adaptation to the state of reception. They will be tested later in the context of the CAPLOC project, supported by the PREDIT program of the French research agency.

The rest of the paper is organized as follows. Section II presents the image analysis step with the description of two proposed methods. Experimental results are shown in Section III. At first, a comparison of the two proposed image analysis methods is given. Based on the satellites repositioning on the processed image, the evaluation of the satellites reception state is then presented. Section IV concludes the paper and presents future works.

II. IMAGE ANALYSIS

In this section, we present a strategy of image analysis to detect the visible sky and other objects present in the image. Many color segmentation methods exist in the literature

D. Attia and C. Meurie and Y. Ruichek are with the University of Technology of Belfort-Montbeliard, Systems and Transportation Laboratory, 13 rue Ernest-Thierry Mieg, 90010 Belfort Cedex, France {dhouha.attia, cyril.meurie, yassine.ruichek}@utbm.fr

J. Marais and A. Flancquart are with the Univ Lille Nord de France, Lille, France - INRETS, LEOST, Villeneuve d'Ascq, France, 20 rue Elisée Reclus, 59650 Villeneuve d'Ascq, France {juliette.marais, amaury.flancquart}@inrets.fr

but few of them guarantee real time constraint. Moreover, we have chosen to consider technique combining color and texture informations since the image of application presents these two informations. Two methods are presented, the first one is based on a segmentation method using an adaptive combination of color and texture information. The second one is based on mathematical morphology and more precisely on a geodesic reconstruction with an optimum parameter of contrast.

A. IMAGE SEGMENTATION COMBINING COLOR AND TEXTURE INFORMATION

In the context of our application, images acquired in mobility present two important informations: color and texture. That is why, we propose a segmentation method based on a non-parametric and adaptive combination of these two informations (see [6] and [7] for more details). This technique uses the watershed algorithm [8], [9] using a specific position of germs and a structural gradient calculated by an intelligent local combination of texture and color information. The texture gradient $Q_{texture}$ can be obtained by different methods: mathematical morphology [10], co-occurrences matrices [11], Gabor filter, etc. The color gradient Q_{color} is generally defined as a color morphological gradient given by: $\delta(f) - \epsilon(f)$ where f is a color image, δ is a dilatation function and ϵ is an erosion function.

The originality of this strategy consists to define a structural gradient combining the texture and color gradients. We start by decomposing the color gradient Q_{color} into its three components, which are Q_{color}^R , Q_{color}^G and Q_{color}^B . In the next step, each component of the color gradient is combined with the texture gradient image $Q_{texture}$. This operation produces three gray level images Q^R , Q^G and Q^B :

$$\begin{cases} Q^R = Q_{col}^R \otimes Q_{tex} \\ Q^G = Q_{col}^G \otimes Q_{tex} \\ Q^B = Q_{col}^B \otimes Q_{tex} \end{cases} \quad (1)$$

Q^R , Q^G and Q^B can be interpreted as the color components of a new color image, which is proposed to define the needed structural gradient. To combine a component of the color gradient q and the texture gradient r , three techniques (fixed, adaptive and supremum combinations) are proposed in our previous works. In this paper, we have chosen to select the supremum combination. Let h be the output of the combination process, which is applied for each pixel.

The proposed supremum combination strategy uses a specific combination of texture and color gradients according to the content of the image. For a given pixel, the structural gradient is a copy of either the color gradient or the texture gradient depending on which one of them provides the biggest amount of information (the supremum). The supremum combination is expressed as follows:

$$h(p) = \begin{cases} q(p), & \text{if } q(p) \geq r(p) \\ r(p), & \text{if } r(p) > q(p) \end{cases}$$

This combination strategy implies two advantages: First, it gives priority to the most important information (the color

or the texture) for a given pixel. Second, it constitutes an automatic (with no parameter) segmentation method, which can perform for all types of images.

Figure 1 illustrates segmentation results obtained by the combination of color and texture information.

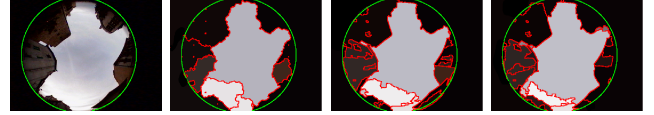


Fig. 1. Initial and segmented images : initial image, segmented image with texture, segmented image with color and segmented image with proposed combination.

B. IMAGE SEGMENTATION USING MATHEMATICAL MORPHOLOGY

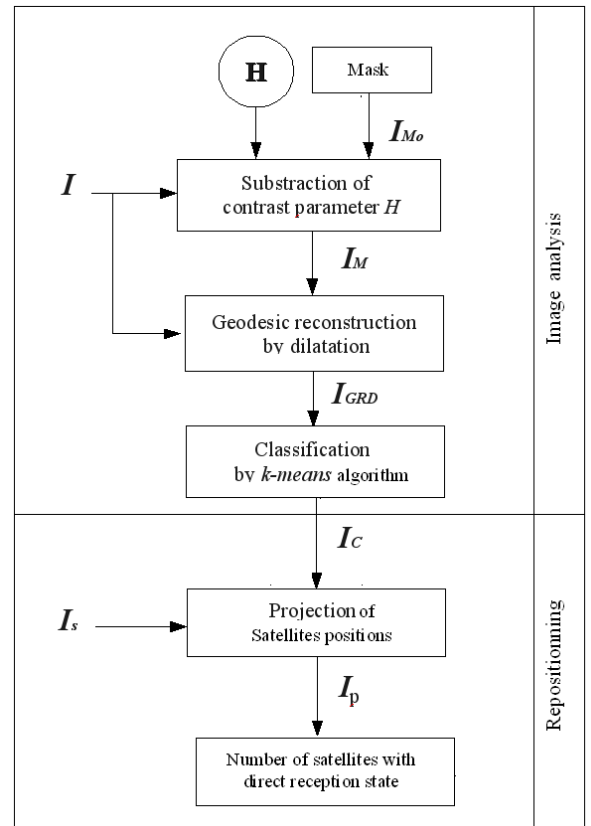


Fig. 2. Global synopsis of the proposed strategy

The color and texture based segmentation technique provides good results. However, its processing rate is very low considering real time applications. In the context of our application, it is very important to diagnostic the satellite state reception in real time. For that, we propose a new strategy of image analysis based on a geodesic reconstruction by dilatation with a low computation time. Figure 2 shows the hole synopsis of the process. Let I be the color image to treat. Let H be the contrast parameter that indicates the

height of peaks to delete. Let I_{M_o} be the mask of the used lens. Used in the geodesic reconstruction, the color image I_M is obtained by subtracting the parameter H at a color component of the initial image I (ie. $I^{C_i} - H \times Id$ where I^{C_i} represents each color component, and Id is the identity matrix). The result of the geodesic reconstruction by dilatation is denoted I_{GRD} . Let I_p be the classified image with satellites positions. The choice of the geodesic operator is explained by his effect of the sky grayscale distribution. Indeed, as we can notice, image acquisition is done in different conditions (illumination variation, lack of stability of the camera due to the movement of the vehicle, etc). One can find obvious variations of sky contrast as for example the presence of clouds in several images that are considered as local peak of grayscale (as illustrated in the third image of Figure 6). For that, it is necessary to homogenize the sky region by a geodesic reconstruction by dilatation. This smoothing operation is helpful for the classification step since it deletes local brilliant peaks. The geodesic operator is expressed as follows:

$$I_{RGD} = \bigvee_{(n \geq 1)} \delta_{I_M}^{(n)}(I) \quad (2)$$

$$\delta_{I_M}^{(n)}(I) = \delta_{I_M}^{(1)} \circ \delta_{I_M}^{(1)} \circ \dots \circ \delta_{I_M}^{(1)}(I) \quad (3)$$

$$\delta_{I_M}^{(1)}(I) = (I \oplus B) \wedge I_M \quad (4)$$

where \oplus corresponds to the morphologic dilatation, B represents the structuring element and $\delta_{I_M}^{(1)}(I)$ is the first rate geodesic dilatation [12]. $\delta_{I_M}^{(n)}(I)$ corresponds to the composition result (denoted by \circ) between the first rate geodesic dilatations until indempotence (given by the n^{th} rate).

In order to optimize the value of the contrast parameter H (that gives the best smoothing of sky region), we perform an exhaustive research on a dataset, which is composed with ten images acquired in different environments (urban and rural) as illustrated in Figure 6. Figure 3 shows the results of the classification rate according to the parameter H . In this figure, each band (colored differently) corresponds to a value of the contrast parameter H . One can notice, some drops at the first bands (ie. of the first values of H) which can be explained by an insufficiency of H to homogenize the sky region for some images. If we consider all images, one can conclude that the best homogenization is obtained with $H = 100$ (corresponding to H_5 illustrated in purple in Figure 3).

Figure 4 illustrates results of a geodesic reconstruction by dilatation with different values of the contrast parameter.

After the image segmentation stage, the second step consists to apply the k-means classification algorithm in order to classify the different region of interest in the image (sky region and not sky region composed with building, vegetation, etc). The classified image is denoted I_C (see Figure 2). The third step consists of repositioning the satellites in the

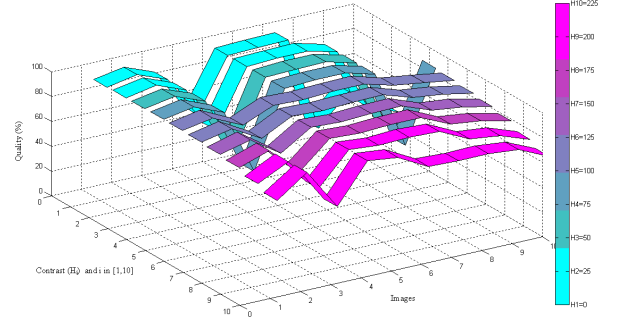


Fig. 3. Quality of the classification according to the contrast parameter $H \in [0, 255]$



Fig. 4. Geodesic reconstruction according to the contrast parameter H (left to right: original image, GRD with $H = 50$, with $H = 100$ and with $H = 150$).

classified image I_C and determining the number of satellites with a direct reception state. To achieve this purpose, we have used both the classified and the original images with the projection of all satellites I_S . This last step is detailed in section III.

III. EXPERIMENTAL RESULTS

In this section, we first present a comparison between the two proposed methods. Then, we explain the method used to replace the satellites in the images. This permits to know if the GNSS signals can be received directly or not by. Before comparing the classification results, we explain the evaluation method providing the percentage of visible sky correctly classified. As stated before, from the segmented image obtained, a classification process is performed using the k-means algorithm. The goal is to classify the image regions into two classes, which correspond to the sky and the rest of the image (vegetation, buildings, ...). For the evaluation, a reference classification is performed for 100 images. Several types of images are used in order to show the influence of experimental conditions of detection results. For example, we can notice images with high illumination (1, 2 and 7) on Figure 6, with dark illumination (4 and 5) on Figure 6 and with clouds (3) on Figure 6. For each classification result, five measurements are computed: 1/ the percentage of pixels that actually make part of the sky region in the classified image and in the reference image; 2/ the percentage of pixels classified as sky but do not make part of the sky region in the reference image; 3/ the percentage of pixels classified as not-sky in both images; 4/ the percentage of pixels classified as not-sky but do not make part of the not-sky region in the reference image; 5/ the fifth measurement, corresponds to the sum of the first and third measurements,

can be viewed as the percentage of pixels that are correctly classified. This percentage corresponds to the quality term used on Y axis of Figure 5 .

A. COMPARISON OF THE IMAGE SEGMENTATION METHODS

In this section, the classification results obtained with the two image segmentation methods (the method combining color and texture information and the method based on the geodesic reconstruction) are compared. To show the interest of performing segmentation before classification, the comparison methodology considers also the classification results obtained directly from the original images using the k-means algorithm. The results are illustrated in Figures 5 (for statistical evaluation) and 6 (for visual classification results on several images). From a quantitative and qualitative point of view (see Fig 5 and 6), one can conclude that the two proposed methods give better results than the k-means algorithm applied directly on the original images. Results obtained by the k-means algorithm are always unsatisfactory and the worse (see third, seventh and tenth images in third line of Figure 6). In average, the method based on the geodesic reconstruction using an optimal contrast parameter H provides results that are almost similar to those obtained with the segmentation method combining color and texture information. For all images of the dataset, the classification rates are 93.1% for the geodesic reconstruction, 89.6% for the combination of color and texture and 73.7% for the k-means algorithm. Furthermore, one can notice that for the image presenting illumination changes (see third stroke of the image 8 in Figure 5, which is illustrated in Figure 6), the proposed method based on the geodesic reconstruction provides the best results. Indeed, one can notice that the geodesic based method provides the best classification results (the sky part is represented in one region. In conclusion, the proposed method based on the geodesic reconstruction by dilatation provides robust and reliable results. In addition, considering the computation time of the strategy that is a fundamental constraint for our application, the method combining texture and color information does not guarantee real time computation. Indeed, this method requires a processing time of about 64 seconds for each image. Considering the method based on the geodesic reconstruction, the processing time is about 0.4 second (with a PC 2.8 GHz, 2Go RAM and an image of size 786x567 pixels), and thus, is compatible with the real time constraint of our application. To conclude this comparison analysis, the geodesic reconstruction based method is chosen to fulfil the task of detection of visible sky.

B. SATELLITES REPOSITIONING

In this section, we present the methodology to replace satellites in the original (fish-eye) images and in the classified ones (Figure 7). After that, we can identify by image analysis satellites that are situated in sky region and satellites that are situated elsewhere. this allows to distinguish the direct state from others ones (blocked, shadowed). The step of satellites

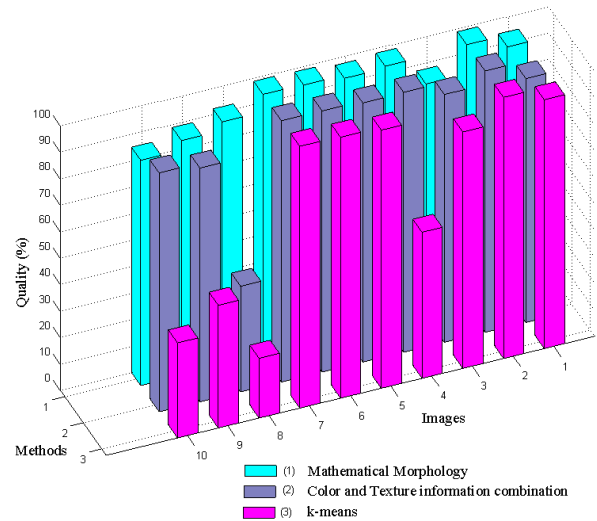


Fig. 5. Comparison between the two proposed approaches (geodesic reconstruction and combination of color and texture information) and a k-means classification algorithm of the litterature.

repositioning consists of three subtasks: 1/ data acquisition; 2/ data calibration and formating; 3/ STK software plateforme.

- Data acquisition: Image acquisition device is composed of a color mono-CCD camera with a fish-eye lens. It is fixed on the vehicle roof and oriented toward the sky. The frequency of the image acquisition is swinging by an odometer that authorizes a regular sampling of the environment. In parallel, NMEA frames acquired by a set of receivers and a Septentrio antenna are saved.
- Data calibration and formatting: We notice that the original images present a distortion phenomenon. This aberration is due to optical properties of fish-eye lens and appears as deformations in the image. To correct this distortion, we perform to a calibration process which consists of matching points of the image with specific points of the real world. Indeed, it is really important to replace the satellite in the image with a precision of one pixel. The classical calibration techniques are not suitable when a large field of view is considered. This is the case when fish-eye lens is used as in our application. Thus, a specific calibration technique is developed to reduce distorsion in fish-eye images.
- STK software: GPGGA frames extracted from NMEA data give each second information about the position of the instrumented vehicle. Associated temporary informations allow to reposition the data of positioning and the images. For a given trajectory and date, the STK software plateforme generates the position for one or many satellite constellations along the trajectory. In the scope of our study, the output file describes the evolution of each satellite position of (GPS and EGNOS constellations). These informations are then replaced in each image.

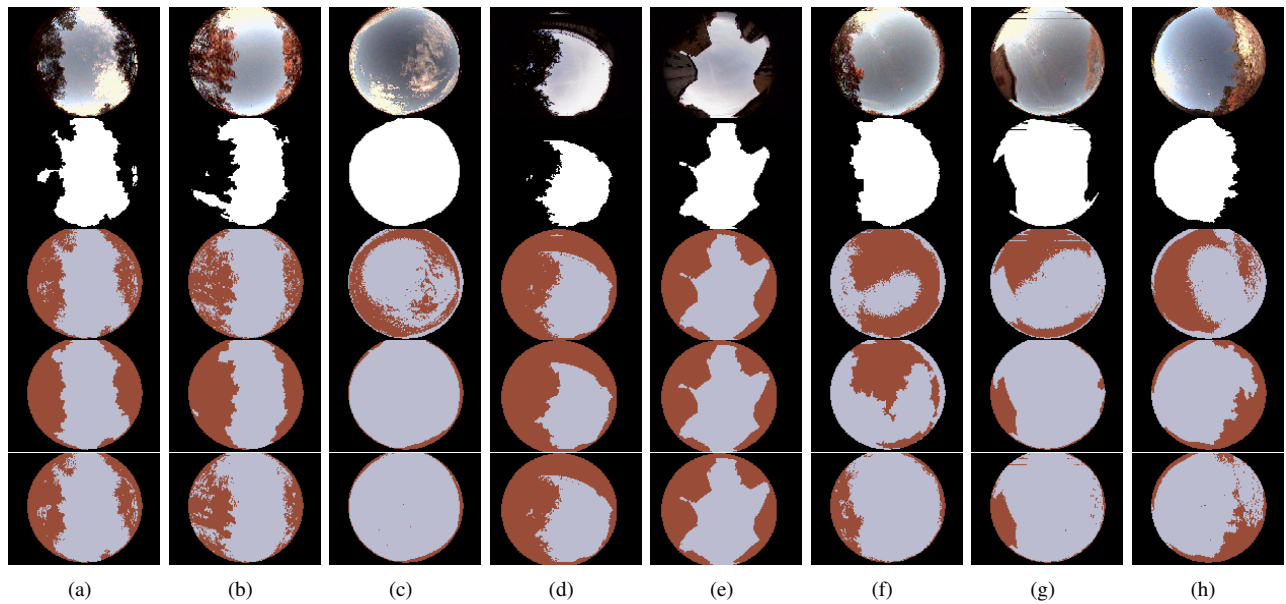


Fig. 6. Classification results obtained by three different methods (top to bottom: original images, reference classification, k-means classification, method combining texture and color information, method based on geodesic reconstruction).

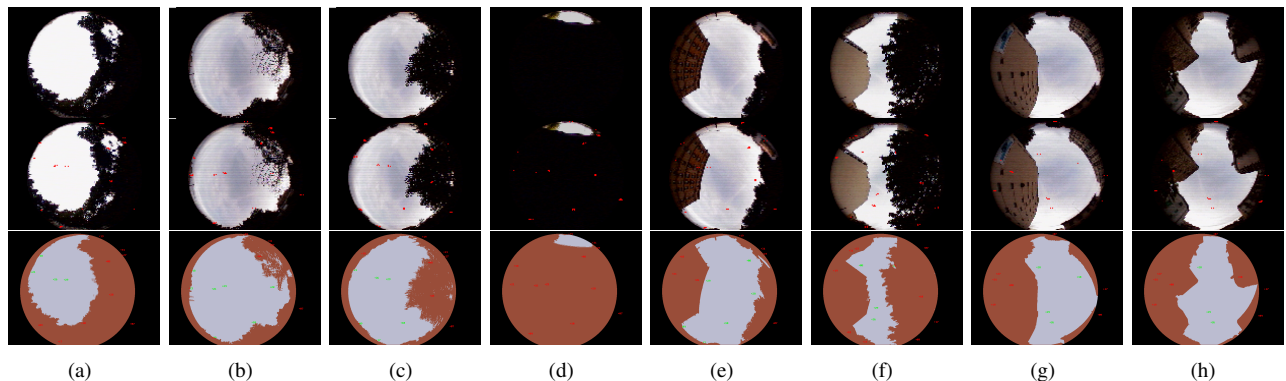


Fig. 7. Reception state of the satellites (top to bottom: original images, original images with satellites position (in red color), classified images with a direct (in green color) and a blocked/shadowed (in red color) reception state).

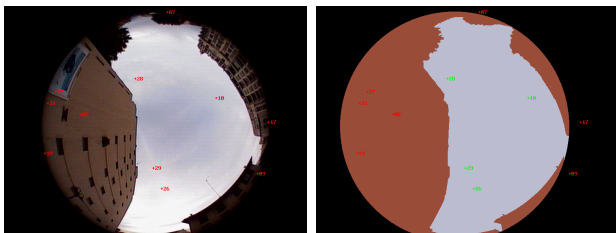


Fig. 8. Zoom on the seventh image with satellites positions (left to right: original image, classified image).

C. SATELLITES RECEPTION STATE

From the previous steps, we determine the number of satellites that have a direct reception state. For that, the original and classified images with the satellites position are used to determine the satellites placed in a sky region (with a direct reception state) and the satellites placed elsewhere (with a blocked or shadowed reception state). The evaluation process is performed using real dataset representing 100 images with

TABLE I
OCCURRENCE SATELLITES WITH DIRECT RECEPTION STATE

Satellites with direct reception state	Occurrence in the dataset
One	16 %
Two	0 %
Three	50 %
Four	16 %
Five	16 %

different difficulties to demonstrate the effectiveness and the reliability of the proposed approach. Figures 7 and 8 and Table I illustrate the final results. In Figure 7, eight various examples of the dataset are presented. One can notice a rural environment (images 7(a), (b) and (c)), an end of tunnel (image 7(d)), an environment with buildings and vegetation (images 7(e) and (f)) and finally a urban environment (images 7(g) and (h)). The first row represents original images and the second one represents the original images with the satellites position (in red). The third row represents the classified im-

ages (the sky region is represented in blue and the obstacles in brown) with the reception state of each satellite (direct in green and blocked or shadowed in red). In images 7(b), (e), (f) and (g), one can see four satellites detected in direct reception state allowing a positioning computation. In images 7(a), (c) and (h), one can notice only three satellites with direct reception state, conducting probably to an inaccurate positioning computation (in this case, the time information is estimated by the receiver). In the fourth image, we have no satellites in direct reception state due to the fact that the environment corresponds to the end of tunnel. Table I illustrates the results obtained for all images of the dataset.

IV. CONCLUSIONS AND FUTURE WORKS

A real time detection of the satellites reception state is presented. The proposed strategy is based on the characterization of the GNSS signals reception environment by image analysis. It consists of detecting the regions of the image that correspond to the sky. For that, a new technique based on a geodesic reconstruction proposed and added to a k-means classification. This technique provides very good classification results compared to the k-means algorithm applied to the original images and to the color and texture information based method (93.1% VS 73.7% and 89.6%). The classification results obtained with this geodesic reconstruction based method are almost unchanging in despite of the content of the image (building, vegetation, tunnel, etc). Furthermore, this method allows a real time processing with a processing rate of about 0.4 second per image. The classification results are then used for satellites repositioning in the image, and thus, the satellites with a direct reception state and those with blocked or shadowed signals are determined. The classification rate (93.1 %) is sufficient now but several classifier types will be used in future works to increase the robustness of the proposed method. Future works concern the estimation of the confidence of positioning computation according to the number of satellites with direct and shadowed signals.

ACKNOWLEDGMENTS

This research work is developed in the framework of the ViLoc project, supported by the Regional Council of Franche-Comté (France).

REFERENCES

- [1] H.-P. Lin, R. Akturan, and W.-J. Vogel, "Satellite-pcs channel simulation in mobile user environments using photogrammetry and markov chains," *Wireless Networks*, vol. 3, pp. 299–308, 1997.
- [2] J. Marais, M. Berbineau, J.-P. Ghys, and M. Heddebaut, "Effect of multipath on availability of gps satellites," in *International Communications Satellite Systems Conference (ICSSC)*, May 2002.
- [3] J.-I. Meguro, T. Murata, J.-I. Takiguchi, Y. Amano, and T. Hashizume, "Gps accuracy improvement by satellite selection using omnidirectional infrared camera," in *IEEE/RSJ International Conference on Intelligent Robots and Systems*, Sept. 2008, pp. 22–26.
- [4] —, "Gps multipath mitigation for urban area using omnidirectional infrared camera," *IEEE Trans. On Intelligent Transportation Systems*, vol. 10, no. 1, pp. 22–30, Mar. 2009.
- [5] A. Rabaoui, N. Viandier, J. Marais, and E. Duflos, "Using dirichlet process mixtures for the modelling of gnss pseudorange errors in urban canyon," in *ION-GNSS*, Sept. 2009, pp. 22–25.

- [6] A. Cohen, C. Meurie, Y. Ruichek, J. Marais, and A. Flancquart, "Quantification of gnss signals accuracy: an image segmentation method for estimating the percentage of sky," in *IEEE International Conference on Vehicular Electronics and Safety (ICVES)*, Nov. 2009, pp. 40–45.
- [7] C. Meurie, Y. Ruichek, A. Cohen, and J. Marais, "An hybrid an adaptive segmentation method using color and textural information," in *IS&T/SPIE, Electronic Imaging 2010 - Image Processing: Machine Vision Applications III*, Jan. 2010.
- [8] L. Vincent and P. Soille, "Watersheds in digital spaces : an efficient algorithm based on immersions simulations," *IEEE Trans. On Pattern Analysis and Machine Intelligence (PAMI)*, vol. 13, no. 16, pp. 583–598, 1991.
- [9] S. Beucher, "Watershed, hierarchical segmentation and waterfall algorithm," *Mathematical morphology and its applications to image and signal processing*, pp. 69–76, 1994.
- [10] J. Angulo, "Morphological texture gradients. application to colour+texture watershed segmentation," *Proc. of the 8th International Symposium on Mathematical Morphology*, pp. 399–410, Oct. 2007.
- [11] S. W. Zucker and D. Terzopoulos, "Finding structure in co-occurrence matrices for texture analysis," *Computer Graphics and Image Processing*, vol. 12, pp. 286–308, 1980.
- [12] L. Vincent, "Morphological gray scale reconstruction in image analysis: Applications and efficient algorithms," *IEEE TRANSACTIONS ON IMAGE PROCESSING*, vol. 2, pp. 176–201, 1993.